BIOCHEMISTRY
including biophysical chemistry & molecular biology

Article

pubs.acs.org/biochemistry

Following DNA Chain Extension and Protein Conformational Changes in Crystals of a Y-Family DNA Polymerase via Raman Crystallography

Shirly J. Espinoza-Herrera,[†] Vineet Gaur,[‡,§] Zucai Suo,[‡] and Paul R. Carey*[,†]

[†]Department of Biochemistry, Case Western Reserve University, Cleveland, Ohio 44106, United States

[‡]Department of Chemistry and Biochemistry, The Ohio State University, Columbus, Ohio 43210, United States

Supporting Information

ABSTRACT: Y-Family DNA polymerases are known to bypass DNA lesions *in vitro* and *in vivo*. *Sulfolobus solfataricus* DNA polymerase (Dpo4) was chosen as a model Y-family enzyme for investigating the mechanism of DNA synthesis in single crystals. Crystals of Dpo4 in complexes with DNA (the binary complex) in the presence or absence of an incoming nucleotide were analyzed by Raman microscopy. ^{13}C- and ^{15}N-labeled d*CTP, or unlabeled dCTP, were soaked into the binary crystals with G as the templating base. In the presence of the catalytic metal ions, Mg^{2+} and Mn^{2+}, nucleotide incorporation was detected by the disappearance of the triphosphate band of dCTP and the retention of *C modes in the crystal following soaking out of noncovalently bound C(or *C)TP. The addition of the second coded base, thymine, was observed by adding cognate dTTP to the crystal following a single d*CTP addition. Adding these two bases caused visible damage to the crystal that was possibly caused by protein and/or DNA conformational change within the crystal. When d*CTP is soaked into the Dpo4 crystal in the absence of Mn^{2+} or Mg^{2+}, the primer extension reaction did not occur; instead, a ternary protein·template·d*CTP complex was formed. In the Raman difference spectra of both binary and ternary complexes, in addition to the modes of d(*C)CTP, features caused by ring modes from the template/primer bases being perturbed and from the DNA backbone appear, as well as features from perturbed peptide and amino acid side chain modes. These effects are more pronounced in the ternary complex than in the binary complex. Using standardized Raman intensities followed as a function of time, the C(*C)TP population in the crystal was maximal at ~20 min. These remained unchanged in the ternary complex but declined in the binary complexes as chain incorporation occurred.

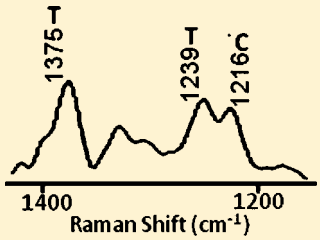

DNA polymerases perform a diverse repertoire of biological functions, including genomic replication, DNA damage repair, lesion bypass, and immunoglobulin diversification. So far, six families of DNA polymerases (A–D, X, and Y) have been classified, and the Y-family established in 2001 is the newest.[1,2] Cellular DNA is frequently damaged by both endogenous and exogenous agents and processes. Although there are various DNA repair pathways, a large number of DNA lesions escape repair and stall replicative DNA polymerases and thus the replication machinery.[3] However, the Y-family DNA polymerases can bypass DNA lesions, thereby rescuing cellular DNA replication. Notably, each living organism contains at least one Y-family DNA polymerase.[2] For example, *Sulfolobus solfataricus*, an aerobic crenarchaeon that metabolizes sulfur and grows optimally at 80 °C and pH 2–4,[4] encodes one Y-family enzyme, DNA polymerase IV (Dpo4).[4,5] In addition to a typical polymerase core with a "right-hand" geometry, consisting of finger, thumb, and palm domains, Dpo4 also contains a fourth domain, designated as the "little finger" (LF) domain[6] (Figure 1).[7] In the ternary structure shown in Figure 1C, the active site of Dpo4 is relatively "loose" and solvent accessible when compared to the active site of a replicative DNA polymerase.[6] Moreover, Dpo4, like all other Y-family DNA polymerases, is devoid of the proofreading exonuclease domain. Thus, Dpo4 catalyzes polymerization in damaged or undamaged DNA with low fidelity.[8−16]

So far, all kinetically characterized DNA polymerases catalyze nucleotide incorporation by following a minimal kinetic mechanism[17] with a rate-limiting precatalytic conformational change.[16−22] Because our recent stopped-flow fluorescence resonance energy-transfer assays conclusively show that a precatalytic global conformational change associated with all four domains of Dpo4 is too fast to be rate-limiting, it was hypothesized that the rate-limiting conformational change corresponds to the subtle repositioning of active site residues that are critical for properly aligning two magnesium ions, the 3′-hydroxyl of the primer terminus, the α-phosphate of the incoming dNTP, and the conserved carboxylate residues within the active site.[19] For the formation of a new phosphodiester bond during nucleotide incorporation, the primer 3′-OH makes an in-line nucleophilic attack on the α-phosphate of an incoming dNTP. Interestingly, the nucleotidyl-transfer reaction catalyzed by a truncated human DNA polymerase η, another Y-family member, has recently been visualized at an atomic level

Received: April 26, 2013
Revised: July 1, 2013
Published: July 3, 2013

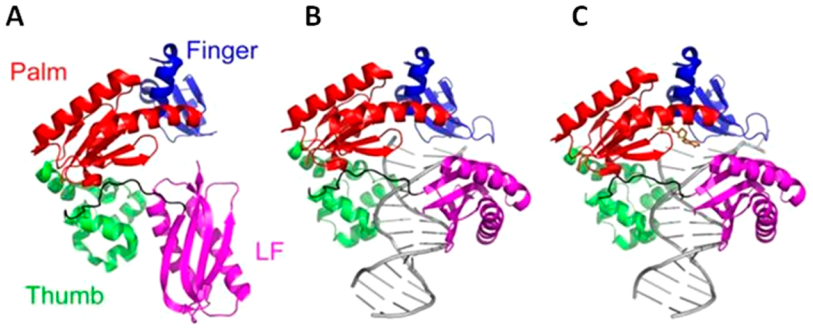

Figure 1. Crystal structure of the (A) apo, (B) binary, and (C) ternary complexes of Dpo4. These structures are presented in ref 7 [Protein Data Bank (PDB) entry 2RDJ]. The linker, DNA, and dNTP are colored black, gray, and orange, respectively.

through time-resolved X-ray crystallography.[23] Previously, the large fragment of *Bacillus stearothermophilus* DNA polymerase I was found to catalyze several rounds of nucleotide incorporation in crystals.[24] Here, single-crystal Raman spectroscopy is employed to probe Dpo4-catalyzed DNA chain extension and relevant protein/DNA conformational changes within crystals.

The Raman method uses a Raman microscope that consists of an optical microscope that allows the operator to view a single crystal within a drop of holding solution mounted in a crystallization tray. A laser excitation beam travels on the optical axis of the microscope and is focused within the single crystal.[25] Back-scattered light from the focal volume travels back through the microscope and is carried by an optical fiber to a Raman spectrometer. The spectrometer provides a Raman spectrum from the focal volume. The basic experiment involves recording the spectrum of the Dpo4·DNA crystal and then adding the ligand/substrate to the drop that contains the crystal. The ligand soaks in the crystal, and the Raman difference spectrum of [Dpo4·DNA + ligand] minus [Dpo4·DNA] reveals chemical details of the reaction between the ligand and the Dpo4·DNA complex.

EXPERIMENTAL PROCEDURES

The DNA polymerase Dpo4 contains 352 amino acids and has an approximate molecular mass of 40 kDa. The enzyme was purified as described previously[15] and cocrystallized with the DNA substrate prepared by annealing a 13-mer DNA primer and an 18-mer template strand shown in Scheme 1 following a published protocol.[6] The DNA strands were purchased from Integrated DNA Technologies, Inc. Single crystals of the Dpo4·DNA complex were grown as described and suspended in a 5 μL hanging drop within a crystallization tray mounted on the stage of a Raman microscope.[25,26] Typically, crystals of the Dpo4·DNA complex had dimensions of 500 μm × 150 μm × 150 μm, and the excitation laser beam was focused through a flat 500 μm × 150 μm face.

2′-Deoxycytidine 5′-triphosphate (dCTP), thymidine 5′-triphosphate, and ^{15}N- and ^{13}C-labeled dCTP (d*CTP) were purchased from Sigma-Aldrich.

The Raman measurements were performed with the 647.1 nm line of a krypton laser; the laser power at the sample was 100 mW, and the spectral data acquisition time was 100 s. Usually, a difference spectrum, the mathematical difference of two spectra, after and before the ligand had been soaked into the crystal, was used to obtain the data.

Scheme 1. DNA Template and Primer Sequence[a]

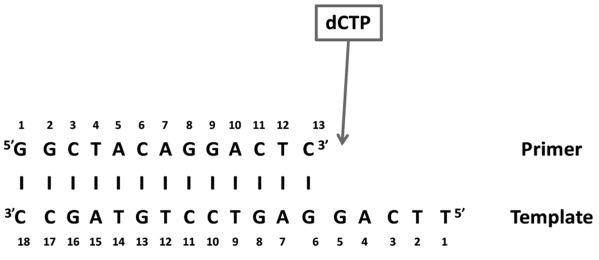

[a]The incoming dCTP will be added to observe the binding and/or nucleotide incorporation reaction.

RESULTS

Raman Spectrum of a Dpo4 Single Crystal. A Raman spectrum of the crystalline DNA·enzyme complex is shown in Figure 2, where a signal-to-noise ratio of ∼140:1 was achieved. This was the highest spectral quality obtained because adding ligand (e.g., dCTP) to the crystals resulted in the deterioration in crystal morphology as is discussed in the next section. In Figure 2, the most intense features are due to well-documented protein modes, e.g., amide I and III, and the aromatic amino acid side chains of Phe and Tyr.[27] However, the four bases of DNA also make a significant contribution, as does the PO_2^- stretch of DNA backbone groups at 1094 cm^{-1}, and the phosphodiester backbone has a stretching mode that contributes to the intensity at 784 cm^{-1}. These assignments are listed in Table 1 and based on refs 27−32. In Figure 2, the amide I feature at 1663 cm^{-1}, the high intensity in the 1340 cm^{-1} region, and the peak at 939 cm^{-1} attest to the presence of significant α-helix structure.[27,31,32] This is consonant with the X-ray crystal structure that has 48% α-helix secondary structure. One band at 1058 cm^{-1} could not be assigned with certainty. Tentatively, this may be a mode from part of the DNA phosphodiester backbone that it is distorted away from the classic A or B form; we have published data on a RNA polymerase that shows features at 1000−1100 cm^{-1} that are assigned to distorted regions of DNA or DNA−RNA duplexes.[32]

Raman Intensity Changes. In the Raman difference spectra discussed below, intensity changes in spectral features that have been assigned to dCTP, d*CTP, or protein and DNA modes from the Dpo4·DNA complex are monitored. There are three sources of intensity changes. (a) For dCTP (d*CTP), the intensity changes are caused by the population changes of the cytosine ring and the attendant triphosphate group inside the crystal. (b) Because the crystal forms a fixed set of axes, Raman dichroism can occur. This happens when groups undergo changes in orientation in the crystal and thus changes in

dx.doi.org/10.1021/bi400524h | *Biochemistry* 2013, 52, 4881−4890

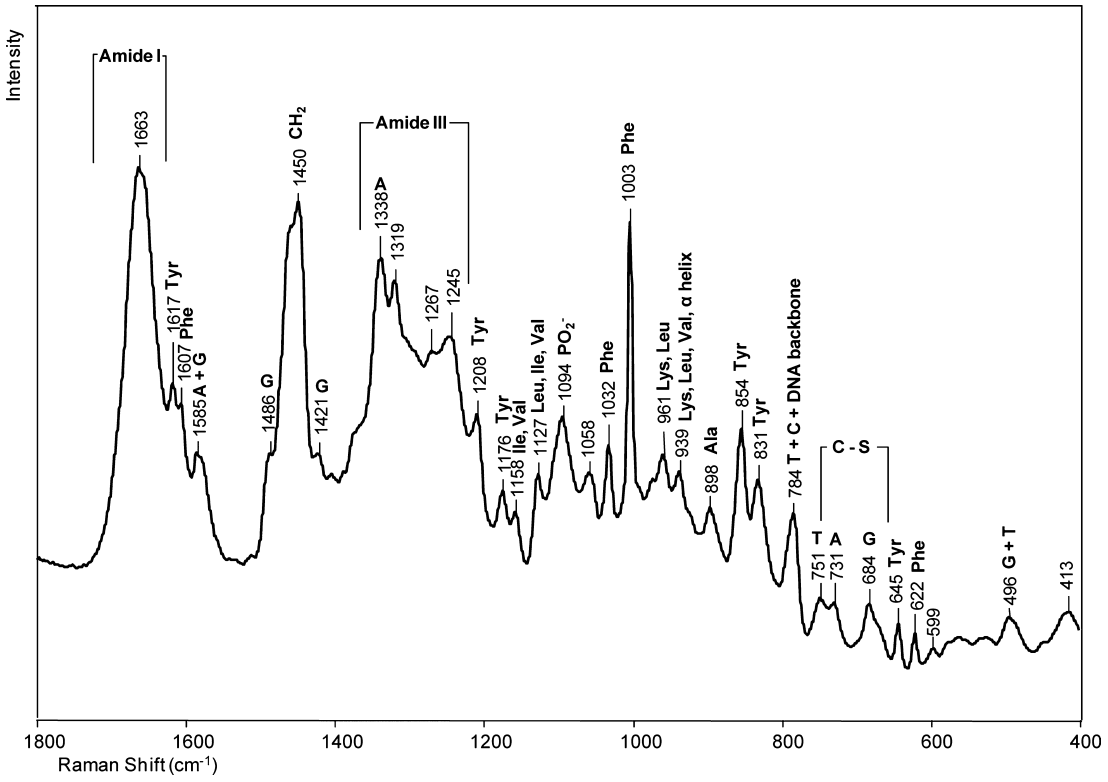

Figure 2. Raman spectrum of a crystal of the binary complex of Dpo4 in a hanging drop containing 100 mM CaAc, 100 mM HEPES, 2.5% glycerol, and 12% PEG 3350 (pH 6.5).

orientation with respect to the fixed orientation of the laser beam. For example, if purine and/or pyrimidine rings undergo a change in orientation during the experiment, the intensity of their Raman modes will change. It is maximal when the rings are at right angles to the incoming laser beam and minimal when the laser beam is parallel to the plane of the ring. This phenomenon is seen predominantly for base ring modes and amide I (mostly C═O) protein modes. (c) When adjacent purine and pyrimidine base modes stack or unstack, this also affects their inherent Raman intensity. By analogy to absorbance spectroscopy, the changes in Raman intensity are termed Raman hypo- or hyperchromism.[27]

Adding d*CTP to the Hanging Drop To Form a Ternary Complex in the Dpo4 Crystal. A ternary complex consists of a protein, a DNA substrate, and an incoming dNTP at the preinsertion stage. If the dNTP becomes covalently linked to the primer via formation of a phosphodiester bond, the result is a postinsertion binary stage. Scheme 2, adapted from ref 33, illustrates the reaction mechanism. Ternary complexes were formed by soaking ^{15}N- and ^{13}C-labeled dCTP (d*CTP) into the crystal in the absence of Mg^{2+} or Mn^{2+} ions using the active template when it will bind in the active site without phosphodiester bond formation.

Spectra at different times for "soaking in" d*CTP are shown in Figure 3A. The main d*CTP ring modes occur at 1215 and 763 cm^{-1} (the d*CTP Raman spectrum in aqueous solution is shown in Figure 5A) with a less intense mode at 1482 cm^{-1}. In Figure 3A, these peaks "grow in" with time (see below). An intense peak remains at 1126 cm^{-1} due to the d*CTP's triphosphate, confirming that the d*CTP has not been incorporated into the primer chain. It must be kept in mind that the d*CTP peaks seen in Figure 3A could contain a contribution from nonspecifically bound ligand [i.e., not H-bonded to template G in the active site (see Scheme 2)] as well as d*CTP correctly bound in the active site. It is also likely that nonspecifically bound d*CTP contributes to the intensity changes seen in Figure 3 by perturbing groups within the Dpo4·DNA complex.

In Figure 3A, several peaks due to dA and dG are identified. These are likely due to the adenine (dA4) in the template next to dG5 that H-bonds to the incoming *dCTP ring and the two guanines in the template closest to the bound d*CTP (dG5 and dG6) (Scheme 1). The formation of the Watson−Crick base pair changes the environment of the neighboring dA4, dG5, and dG6 and, hence, the intensity of the ring modes. Because this is a fixed population, the intensity changes are probably the effect of Raman dichroism, although Raman hyper- or hypochromism may play a role.[27] Other notable bands in Figure 3A come from amide I modes at 1671 and 1653 cm^{-1} and amide III modes at 1295 and 1254 cm^{-1}. Raman dichroism is likely responsible, although changes in protein secondary structure may occur upon addition of d*CTP. The intensity of the amide I modes in Figure 3A at 37 min is ∼8% of the intensity of the amide I mode in Figure 2. This implies that the change seen in Figure 3A is equivalent to the intensity of 0.08 times the total number of amino acids, 352, namely 29 amino acids. The amide intensity change in Figure 3A is equivalent to 29 amino acids. To generate this value, it means that more than 29 amino acids have moved and undergone changes in amide I intensity in the ternary compared to the binary complex. Possibly, the d*CTP in the active site is causing dynamic protein fluctuations to be damped, leading to a slight narrowing of the amide I profiles, and this could be another cause of the apparent increase in amide I and III mode intensities. In Figure 3A, the appearance of the band at 785 cm^{-1} is due to a backbone phosphodiester

dx.doi.org/10.1021/bi400524h | Biochemistry 2013, 52, 4881−4890

Table 1. Raman Peak Assignments for a Crystal of the Dpo4·DNA Complex[a]

Raman peak (cm^{-1})	Assignment
1663	amide I
1617	Tyr
1607	Phe
1585	A, G
1486	A, G
1450	δCH_2
1421	G
1240−1300	amide III
1338	A
1208	Tyr
1176	Tyr
1158	Ile, Val
1127	Leu, Ile, Val
1094	PO_2^-
1058	DNA phosphodiester backbone
1032	Phe
1003	Phe
961	Lys, Leu
939	Lys, Leu, Val, α-helix
898	Ala
854	Tyr
831	Tyr
784	C, T, DNA phosphodiester backbone
751	T
740−680	C−S
731	A
684	G
645	Tyr
622	Phe
496	G, T

[a]The assignments are based on refs 27−32.

Scheme 2. Reaction Mechanism of a DNA Polymerase

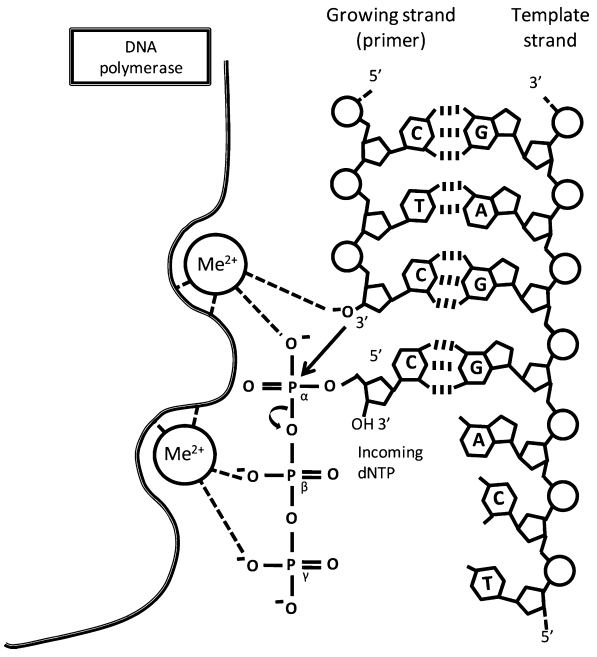

stretch mode of DNA, and this represents 19% of the intensity of the 785 cm^{-1} band in Figure 2. This indicates that the DNA backbone has undergone a significant conformational change in the ternary complex. The Raman data by themselves do not usually identify the specific locations of the observed protein and DNA changes.

In Figure 4, the intensities of the Raman peaks are plotted during soak-in using the inactive template that is dideoxy at the 3′-C in the presence of 50 mM Mn^{2+}. The peak heights are standardized with the Phe peak at 1004 cm^{-1} in the mother spectrum prior to subtraction. For marker bands, the following features are used: for triphosphate near 1120 cm^{-1}, C at 1241 cm^{-1}, and DNA phosphodiester backbone at 784 cm^{-1}. All these marker bands show a similar time dependence, and the changes in intensity are ascribed predominantly to population changes. This is an initial fast phase from 0 to ∼20 min corresponding to the maximal C(*C)TP population. This is followed by a plateau with possibly a small increase in intensity from 20 to 100 min, which was the limit of the crystal stability. In Figure 3, for d*CTP, at 19 min soak-in the difference spectrum is dominated by d*CTP features but by 37 min has more contribution assigned to template nucleic acid and protein features. At 37 min, the *C peak intensities are essentially unchanged from those at 19 min. However, the increase in amide III intensity at 1254 cm^{-1} and in ring modes associated with the nucleic acid scaffold suggests that slow conformational changes occur after the point where the maximal *C population is reached.

When "soak-in" experiments were conducted with the Dpo4 binary complex, crystal cracking was invariably observed. Factors that may contribute to the cracking are protein and/or DNA conformational changes that, due to crystal packing forces, are not allowed the freedom to complete the changes that would be seen in solution. This would lead to unfavorable protein−protein constraints in the crystal that can be relieved by crystal fragmentation.

The spectrum in Figure 3B is obtained under "soak-out" conditions. After d*CTP had been "soaked in" for 120 min, the crystal was transferred to a holding solution that contained neither d*CTP, Mg^{2+}, nor Mn^{2+}. The difference spectrum was obtained after "soak-out" conditions had been emplyed for 40 min. The trace is almost a straight line showing that the d*CTP has left the crystal completely because no d*C ring modes remain. Moreover, the dA modes from the template disappear, showing that the dA ring has resumed its position that is identical to that of the dA prior to d*CTP being soaked in. Only very weak features persist. These are attributed to Tyr and Phe side chain modes and to the template dG ring closest to the d*CTP binding site that have not relaxed back completely to their prebinding state after 40 min. The same conclusion can be drawn for the DNA backbone giving rise to the negative phosphodiester mode at 785 cm^{-1}. The change in the DNA backbone is greatly diminished after "soak-out".

Extending the DNA Chain by One Base by Soaking in dCTP in the Presence of a Divalent Metal Ion. To promote chain extension within the crystal, 50 mM Mn^{2+} ions (50 mM $MnCl_2$)[34] were added to the holding solution containing the crystal before 10 mM unlabeled dCTP was soaked in. The resulting difference spectra are shown in Figure 6. At the 62 min soak-in point, the spectrum seen in Figure 6A was obtained. The most intense peaks due to dC ring modes (see Figure 5B for the spectrum of aqueous unlabeled dCTP) are seen at 1529, 1293, 1255, and 785 cm^{-1}. The medium-intensity peak at 1122 cm^{-1} is due to dCTP's triphosphate and is evidence that some unreacted dCTP remains in the crystal.

dx.doi.org/10.1021/bi400524h | Biochemistry 2013, 52, 4881−4890

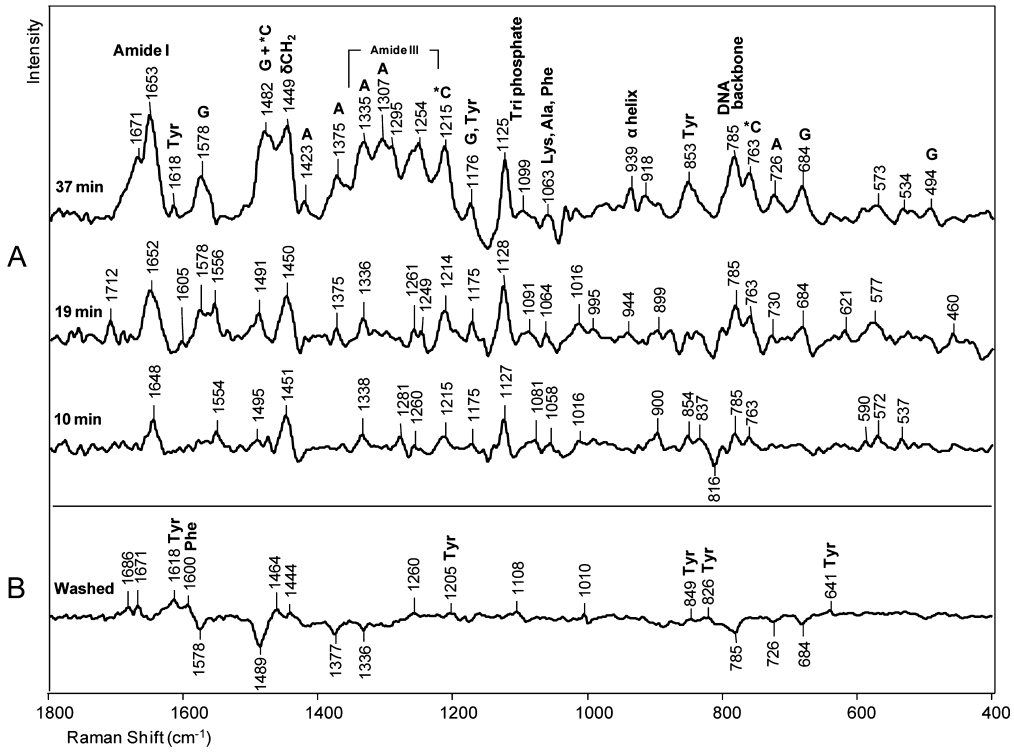

Figure 3. Ternary complex formation. Raman difference spectra of a crystal of Dpo4 in a hanging drop with no Mg^{2+} or Mn^{2+} ions. (A) Raman spectra of the crystal different periods of time (10, 19, and 37 min) after the addition of 4 mM d*CTP to the hanging drop minus the Raman spectrum before the addition of d*CTP. (B) Raman spectrum after the crystal had been washed for 40 min in the initial holding solution without d*CTP minus the Raman spectrum before the crystal had been soaked in d*CTP.

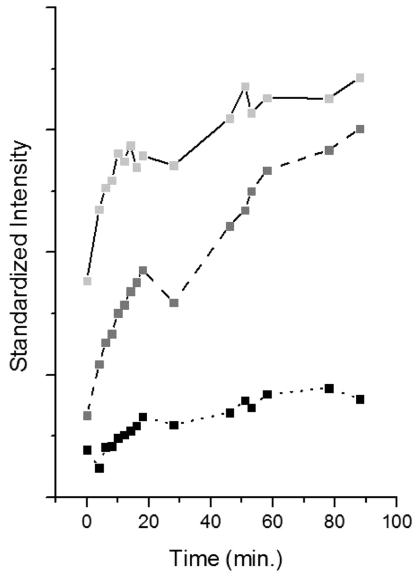

Figure 4. Ternary kinetics. dCTP (10 mM) was added to a holding solution containing Dpo4·DNA crystal with an inactive template and 50 mM $MnCl_2$. The heights of several peaks rationed to the Phe peak are plotted at different times: (—) 783 cm^{-1} peak assigned to the DNA backbone and C, (---) 1241 cm^{-1} peak assigned to C, and (···) 1116 cm^{-1} peak assigned to triphosphate.

Many bands are assigned to dA and dG ring modes, and these result from dCTP perturbing the environment of the bases on the primer and template, as in the ternary complex discussed in the previous section. Similarly, binding brings about changes in the Tyr side chain environment, evidenced by the "negative" 856 cm^{-1} feature, and Tyr10 and Tyr48 in the active site are good candidates for being the source of this change. The broad feature near 1658 cm^{-1} is due to Dpo4's amide I modes and shows that some perturbation of the protein α-helical secondary structure has also occurred, although distinct amide III modes are not observed. The intense band at 785 cm^{-1} owes its intensity to a dC ring mode. Although a DNA backbone mode occurs at the same position, it is unlikely that it contributes significantly because the insert band for *CTP shows weak intensity at 783 cm^{-1}. Some of the intensity between 1030 and 1100 cm^{-1} is likely due to phosphodiester modes.[32] For example, the peak at 1094 cm^{-1} is due to the PO_2^- groups of the DNA backbone, and this is evidence that the reaction is occurring because chain extension adds one additional PO_2^- to the chain.

Features due to pyrophosphate could not be unambiguously detected. The Raman spectra of pyrophosphate tetrabasic ($Na_4P_2O_7$) in water over a range of pHs are shown in Figure S1 of the Supporting Information. The peaks with the highest intensities are in the region of 1000−1150 cm^{-1}, where PO_2^- modes from the DNA backbone occur and specific peaks due to the formation of pyrophosphate are difficult to identify. The pyrophosphate peak near 716 cm^{-1} (Figure S1 of the Supporting Information) was not observed, possibly because of its relatively low intensity and broadness or the pyrophosphate product leaving the crystal.

In Figure 6A, there are undoubtedly contributions from dCTPs that are not specifically bound in the active site and have not been covalently linked to the primer chain. Thus, "soaking out" was employed. After soaking in had been conducted for 62 min, we placed the crystal in a holding solution that did not contain dCTP (50 mM Mn^{2+} metal

dx.doi.org/10.1021/bi400524h | Biochemistry 2013, 52, 4881−4890

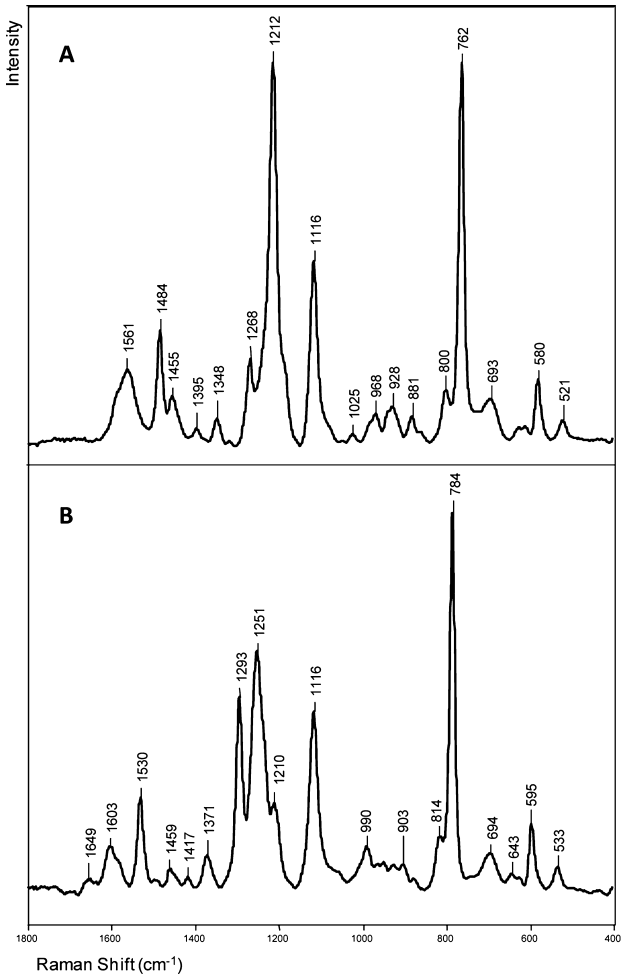

Figure 5. Raman spectra of deoxycytidine triphosphate. (A) Raman spectrum of 100 mM 2′-deoxycytidine-$^{13}C_9$,$^{15}N_3$ (labeled deoxycytidine) 5′-triphosphate (d*CTP) in solution (pH 7.0) in a hanging drop. (B) Raman spectrum of 100 mM 2′-deoxycytidine 5′-triphosphate (dCTP) in solution (pH 7.0) in a hanging drop. Both spectra were recorded using a power of 100 mW, 647.1 nm laser excitation, and data accumulation for 100 s.

remains). After soaking out had been conducted for 30 min, the spectrum in Figure 6B was obtained. The intensity of the dC modes has diminished by ∼65%, showing that approximately one-third of the original dCTPs in the crystal has been incorporated into the primer chain. The triphosphate peak at 1125 cm^{-1} is small, showing that now only a small amount of unreacted dCTP remains. Many perturbations persist, but compared to the ternary complex, changes in the protein conformation are smaller; the broad amide I band at 1658 cm^{-1} (Figure 5A) is replaced by three smaller peaks at 1681, 1667, and 1648 cm^{-1}. These are tentatively assigned, at least in part, to the "C═O modes" from the new G-C Watson−Crick base pair that has been formed.

Figure 7 shows the variation in intensity with time of the *C ring mode under conditions when the reaction is occurring (with the reaction template and 50 mM $MnCl_2$). The population of *C, gauged by the ring mode intensity at 1214 cm^{-1}, increases rapidly to ∼23 min and then decreases. The triphosphate population using the 1119 cm^{-1} mode as a marker also increases rapidly and peaks at 23 min and declines as *CMP is incorporated into the DNA primer strand. The similar maxima in both traces in Figure 7 suggest that catalysis becomes dominant at approximately the point of "full soak-in". The decrease in the *C population in Figure 7 indicates that nonspecifically bound *CTP is expelled from the crystal after incorporation begins at around 23 min and suggests that a conformational change that leads to less favorable binding of nonspecific *CTP is occurring.

It is noteworthy that soaking in dCTP in the presence of 1 mM dCTP and 50 mM Mn^{2+} resulted in only specific binding. The intensities of the cytosine peaks in the difference spectrum after soaking in the crystal in a solution with 1 mM labeled dCTP after 40 min are the same as the intensities of the cytosine peaks after the soaking out experiment (Figure 6B) obtained by washing the crystal for 40 min in a solution without dCTP (data not shown).

There is no way of separating the effects of specific (i.e., *C Watson−Crick binding to template G) and nonactive site d*CTP binding in Figure 3. However, the spectrum in Figure 6A suggests that there are fewer intensity changes for the binary complex with noncovalently bound dCTPs than in Figure 3A for the ternary complex with nonspecifically bound d*CTPs. This is supported by data in Figure 8A that compare covalently labeled d*CTP in a pure binary complex (Figure 6B) with that prior to soak-out where noncovalent d*CTPs are also present. Although the quality of the data is not optimal, in Figure 6B, after soak-out, compared to the ternary complex in Figure 3, only minor changes are seen in the amide I region near 1650 cm^{-1} and the DNA backbone marker band near 780 cm^{-1}. In total, the data suggest that in the binary complex the protein and DNA backbone changes are probably minor compared to those seen in the ternary complex.

Extending the DNA Chain by Two Bases Using d*CTP and dTTP. To obtain a binary complex in which one d*C was added to the primer, we repeated the protocol in the previous section using ^{13}C- and ^{15}N-labeled dCTP (d*CTP). The results are shown in Figure 8A. d*CTP (7 mM) with Mn^{2+} (50 mM) was soaked in for 40 min and then soaked out for 30 min in a holding solution that did not contain d*CTP. Although the quality of the data in Figure 8A are inferior to the quality of those in Figure 6, the spectrum of the washed out crystal resembles closely the spectrum in Figure 6B except that the main dC ring modes are downshifted; e.g., the mode around 785 cm^{-1} is "downshifted" 22 cm^{-1} due to the ^{13}C and ^{15}N substitutions (d*C). Figure 8A confirms that for the binary complex the changes in protein and DNA conformation are small compared to those for the ternary complex because the amide I and III features and DNA backbone feature near 785 cm^{-1} are weak in the difference spectrum. This binary crystal was then soaked in 2 mM dTTP in the presence of 50 mM Mn^{2+} for 100 min. Then, following soaking in dTTP, the crystal was placed in a holding solution that has no dTTP for 50 min; the resulting difference spectrum is seen in Figure 8B. The multiple-soak process gave crystals that had cracked and lost most of their crystalline appearance. However, a difference Raman spectrum that showed both d*C and dT ring modes could be obtained, strongly suggesting that both d*C and dT have been incorporated into the primer chain. No evidence of unreacted triphosphate is seen in Figure 8B.

It is of great interest that intense dA and dG ring modes occur in Figure 8B as does a peak from the DNA phosphodiester backbone at 784 cm^{-1}. The high intensities suggest that upon the second soak with dTTP changes in the primer and/or template are much larger than those seen on the first d*CTP incorporation. This is interpreted as resulting from

dx.doi.org/10.1021/bi400524h | *Biochemistry* 2013, 52, 4881−4890

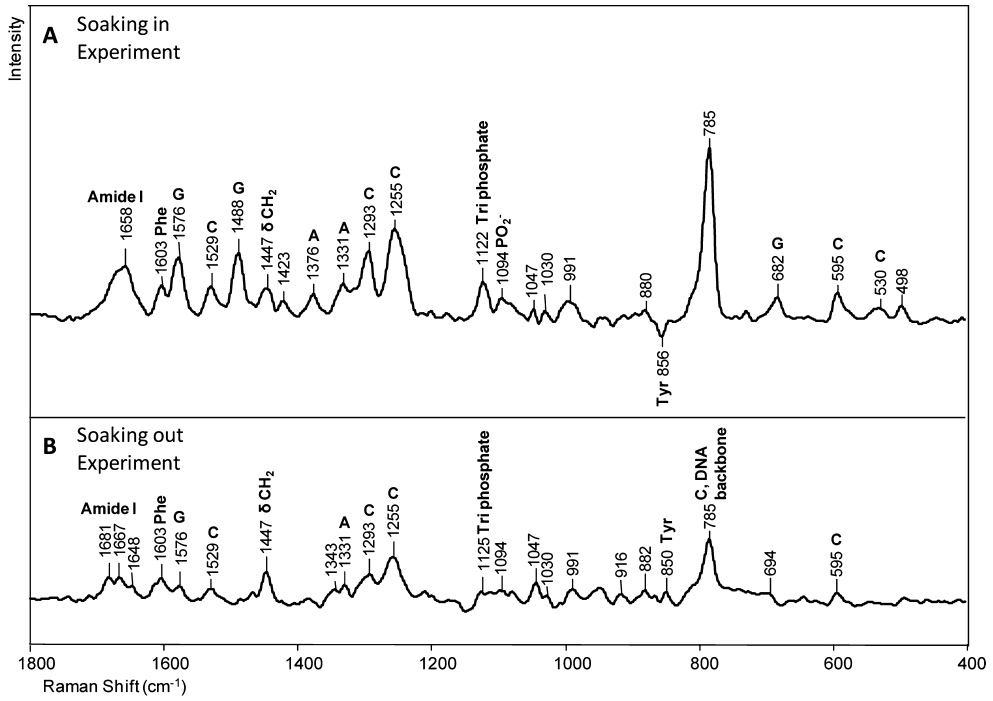

Figure 6. Effect of covalent addition of dCTP to the primer chain. dCTP (10 mM) was added to a crystal of the binary complex of Dpo4 in a hanging drop containing 50 mM $MnCl_2$. (A) Raman difference spectrum 62 min after the addition of 10 mM dCTP to the crystal in the hanging drop minus the Raman spectrum before dCTP had been soaked in. (B) Raman spectrum after the crystal had been washed for 30 min (after the reaction with dCTP) in the initial holding solution without dCTP minus the Raman spectrum before the crystal had been soaked in with dCTP.

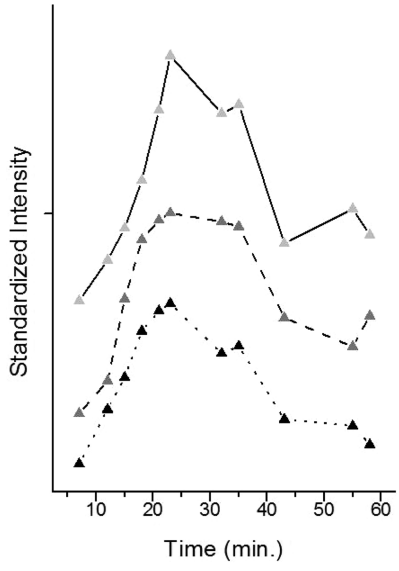

Figure 7. Binary kinetics. d*CTP (1 mM) was added to a holding solution containing a Dpo4·DNA crystal with the active template and 50 mM $MnCl_2$ to start the polymerization reaction. Standardized peak heights are plotted at different times: (—) 762 cm^{-1} and (---) 1214 cm^{-1}, both assigned to labeled C (*C), and (···) 1119 cm^{-1}, assigned to triphosphate.

primer and template translocation, full or partial, through the active site of Dpo4 to bring the template dA base into register with the catalytic machinery.

DISCUSSION

The Raman difference spectra allow us to observe structural and conformational changes in a crystalline Dpo4·DNA complex occurring when the DNA polymerization reaction is catalyzed by the Y-family polymerase Dpo4. The Raman peaks in the difference spectra with the highest intensity are usually caused by the added nucleotide, dCTP, d*CTP, or dTTP, but peaks corresponding to changes in the protein·DNA conformations or template/primer base perturbations can also be observed. For the latter, larger changes are observed in ternary compared to binary complexes. The evidence of chain incorporation of dNTP is based on the fact that the C, *C, or T ring modes remain in the crystal after the noncovalently bound ligands had been extensively "soaked out". This is supported by the observations that there is little evidence of the reactive dNTP triphosphate group after "soak-out". It is noteworthy that Xu et al.[19] proposed that a local active site rearrangement is a rate-limiting conformational change step driving a single-correct dNTP incorporation process. However, their studies were conducted in aqueous solution, and we will need to undertake future rapid mix–rapid quench experiments in solution as detailed below to examine conformational changes on the millisecond time scale.

Running the reaction in the crystal comes at a price. Significant degradation of the crystal morphology is observed. This could prevent future parallel X-ray crystallography experiments that could use the Raman experiments as reference points for flash freezing to conduct time-dependent X-ray analysis.[32,35−37] For future experiments, the approach detailed by Nakamura et al.[23] will be employed; in their study of the reaction of DNA polymerase η from the Y-family, they cocrystallized the substrate and the enzyme in the absence of divalent metal ions, which prevents the chain incorporation reaction from occurring. They then triggered the reaction by soaking in Mg^{2+} and could observe high-resolution maps by flash freezing at different time points during metal "soak-in". It is possible that a major cause of the crystal cracking seen in our

dx.doi.org/10.1021/bi400524h | Biochemistry 2013, 52, 4881−4890

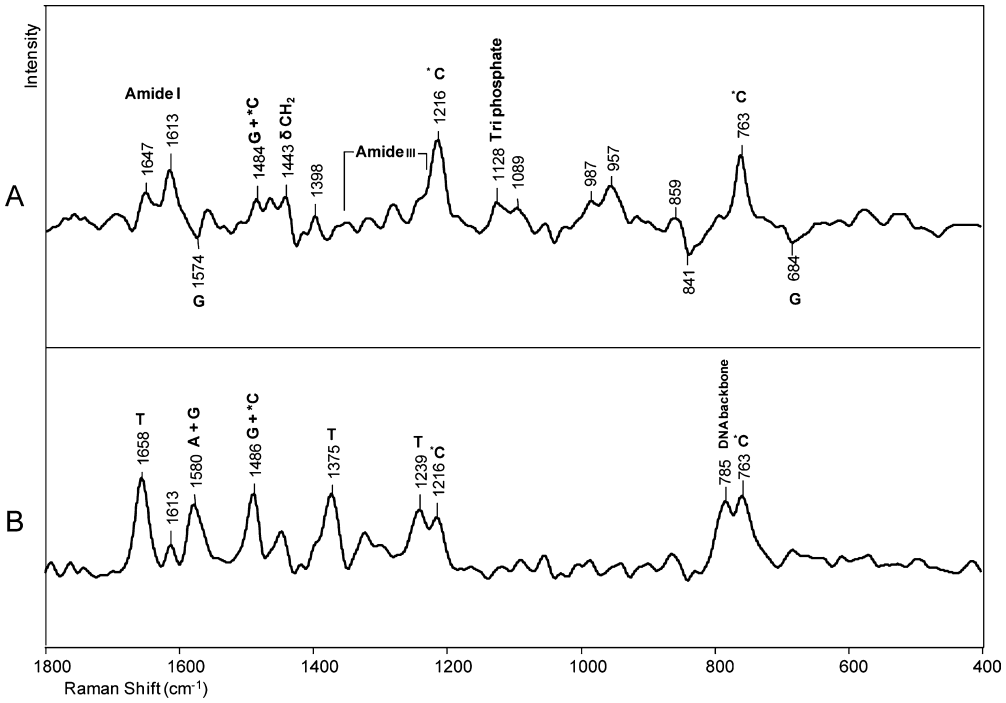

Figure 8. Sequential addition of cytidine and thymidine to the nascent DNA chain. ^{15}N- and ^{13}C-labeled dCTP (d*CTP) (7 and 2 mM, respectively) were added sequentially to a crystal of Dpo4 in a hanging drop containing 50 mM $MnCl_2$. (A) Raman difference spectrum of the crystal after reaction with d*CTP for 30 min minus the Raman spectrum before soaking in d*CTP. (B) Raman difference spectrum showing the dTTP reaction after the addition of d*CTP to the primer chain. dTTP (2 mM) was soaked into the crystal containing covalently bound d*C for 100 min. This crystal was washed for 50 min in a holding solution containing no dTTP. Figure 7B is the difference spectrum [d*C crystal + dTTP + washing] minus [crystal before addition of d*CTP].

experiments is the conformational changes the enzyme wishes to make to achieve translation being opposed by crystal packing forces.

Clearly, it would be of great interest to compare the reaction in solution with that in the crystal. Until very recently, solution studies using normal (nonresonance) Raman spectroscopy were technically impossible. However, a flash freezing protocol that can examine the reaction in aqueous solution on the millisecond time scale has been developed in our laboratory,[38] and this approach will be used to follow dNTP incorporation catalyzed by Dpo4 DNA polymerase in aqueous solution.

Our Raman database of nucleic acid polymerases is being extended. The present DNAP is the smallest, a single subunit of ~40 kDa containing a DNA primer and an 18-nucleotide template. Recently, results for a 115 kDa RNA polymerase from the N4 phage virion were presented after the initiation of the RNA chain had been studied.[39] This *in crystallo* initiation reaction was ~3 times faster than the present DNA chain extension. The simultaneous soak-in of GTP and ATP was observed to plateau at 7 min. A small protein conformational change was seen at approximately the same time, and this was assigned to movement of the α-helix near the active site. Functional active site formation about two Mg^{2+} ions was also seen in <10 min as evidenced by Asp side chains acting as ligands to Mg^{2+}. Triphosphate intensity reduction showed that catalysis was complete shortly after 10 min. Basu and Murakami[40] used the Raman kinetic data to flash freeze and determine the structures of the N4 crystals at time points between 0 and 10 min of soak in. The predictions from Raman crystallography were borne out; they were able to obtain high-quality X-ray structures for intermediates during the formation of the covalent nucleic acid backbone bond. The trio of polymerases is completed by recent Raman studies of a RNAP from the bacterium *Thermus thermophilus* (*Tth* RNAP) (unpublished work, this laboratory). This is a five-subunit 380 kDa "machine". Time-resolved *in crystallo* Raman data showed that the base to be incorporated, GTP, soaks in and "plateaus" after 30 min. This triggers a large reversible change in protein conformation probably from functionally important α-helices that flank the active site to crablike "pincers" that form a channel to the active site. The protein conformational change is accompanied by a modest and reversible change in DNA backbone from the RNA–DNA hybrid between 0 and 60 min. The conformational changes lead to GTP incorporation between 65 and 100 min. Covalent bond formation occurs, apparently, shortly after the nucleic acid skeleton has translocated through the active site channel. Remarkably, the *Tth* RNA polymerase in the crystal appears to be primed for a second round of nucleotide triphosphate incorporation.

Thus, in all these NAPs, the cognate NTP can be followed soaking into its crystal and starting or incorporating into a nucleic acid chain. The time scales range from minutes to tens of minutes, probably 10000 to 100000 times slower than in solution. In each instance, the time points of "interesting intermediates" that are candidates for X-ray analysis can be identified. In the case of RNAP from N4, this prediction has been met and their intermediates have been characterized by X-ray crystallography. DNAP and *Tth* RNAP reactions have yet to be studied by X-ray.

dx.doi.org/10.1021/bi400524h | *Biochemistry* 2013, 52, 4881–4890

■ ASSOCIATED CONTENT

Supporting Information

Raman spectra of pyrophosphate tetrabasic ($Na_4O_7P_2$) in solution as a function of pH (Figure S1). This material is available free of charge via the Internet at http://pubs.acs.org.

■ AUTHOR INFORMATION

Corresponding Author

*Department of Biochemistry, Case Western Reserve University, Cleveland, OH 44106. E-mail: prc5@case.edu. Telephone: (216) 368-0031. Fax: (216) 368-3419.

Present Address

§V.G.: International Institute of Molecular and Cell Biology in Warsaw, 4 Ks. Trojdena Street, 02-109 Warsaw, Poland.

Funding

This work was supported by the National Science Foundation (Grant MCB-0960961 to Z.S.) and National Institutes of Health Grants GM54072 and GM81420 to P.R.C.

Notes

The authors declare no competing financial interest.

■ REFERENCES

(1) Hubscher, U., Maga, G., and Spadari, S. (2002) Eukaryotic DNA polymerases. *Annu. Rev. Biochem. 71*, 133−163.

(2) Ohmori, H., Friedberg, E. C., Fuchs, R. P. P., Goodman, M. F., Hanaoka, F., Hinkle, D., Kunkel, T. A., Lawrence, C. W., Livneh, Z., Nohmi, T., Prakash, L., Prakash, S., Todo, T., Walker, G. C., Wang, Z., and Woodgate, R. (2001) The Y-family of DNA polymerases. *Mol. Cell 8*, 7−8.

(3) Jackson, S. P. (2001) Detecting, signalling and repairing DNA double-strand breaks. *Biochem. Soc. Trans. 29*, 655−661.

(4) She, Q., Singh, R. K., Confalonieri, F., Zivanovic, Y., Allard, G., Awayez, M. J., Chan-Weiher, C. C. Y., Clausen, I. G., Curtis, B. A., De, M. A., Erauso, G., Fletcher, C., Gordon, P. M. K., Heikamp-De, J. I., Jeffries, A. C., Kozera, C. J., Medina, N., Peng, X., Thi-Ngoc, H. P., Redder, P., Schenk, M. E., Theriault, C., Tolstrup, N., Charlebois, R. L., Doolittle, W. F., Duguet, M., Gaasterland, T., Garrett, R. A., Ragan, M. A., Sensen, C. W., and Van der Oost, J. (2001) The complete genome of the crenarchaeon *Sulfolobus solfataricus* P2. *Proc. Natl. Acad. Sci. U.S.A. 98*, 7835−7840.

(5) Prangishvili, D., and Klenk, H. P. (1993) Nucleotide sequence of the gene for a 74 kDa DNA polymerase from the archaeon *Sulfolobus solfataricus*. *Nucleic Acids Res. 21*, 2768.

(6) Ling, H., Boudsocq, F., Woodgate, R., and Yang, W. (2001) Crystal structure of a Y-family DNA polymerase in action: A mechanism for error-prone and lesion-bypass replication. *Cell 107*, 91−102.

(7) Wong, J. H., Fiala, K. A., Suo, Z., and Ling, H. (2008) Snapshots of a Y-Family DNA Polymerase in Replication: Substrate-induced Conformational Transitions and Implications for Fidelity of Dpo4. *J. Mol. Biol. 379*, 317−330.

(8) Masutani, C., Kusumoto, R., Yamada, A., Dohmae, N., Yokoi, M., Yuasa, M., Araki, M., Iwai, S., Takio, K., and Hanaoka, F. (1999) The XPV (xeroderma pigmentosum variant) gene encodes human DNA polymerase *η*. *Nature 399*, 700−704.

(9) Matsuda, T., Bebenek, K., Masutani, C., Hanaoka, F., and Kunkel, T. A. (2000) Low fidelity DNA synthesis by human DNA polymerase *η*. *Nature 404*, 1011−1013.

(10) Johnson, R. E., Washington, M. T., Haracska, L., Prakash, S., and Prakash, L. (2000) Eukaryotic polymerases *ι* and *ζ* act sequentially to bypass DNA lesions. *Nature 406*, 1015−1019.

(11) Levine, R. L., Miller, H., Grollman, A., Ohashi, E., Ohmori, H., Masutani, C., Hanaoka, F., and Moriya, M. (2001) Translesion DNA synthesis catalyzed by human pol *η* and pol *κ* across 1,N6-ethenodeoxyadenosine. *J. Biol. Chem. 276*, 18717−18721.

(12) Bebenek, K., Tissier, A., Frank, E. G., McDonald, J. P., Prasad, R., Wilson, S. H., Woodgate, R., and Kunkel, T. A. (2001) 5′-Deoxyribose phosphate lyase activity of human DNA polymerase *ι* in vitro. *Science 291*, 2156−2159.

(13) Zhang, Y., Yuan, F., Xin, H., Wu, X., Rajpal, D. K., Yang, D., and Wang, Z. (2000) Human DNA polymerase *κ* synthesizes DNA with extraordinarily low fidelity. *Nucleic Acids Res. 28*, 4147−4156.

(14) Wang, Z. (2001) Translesion synthesis by the UmuC family of DNA polymerases. *Mutat. Res., DNA Repair 486*, 59−70.

(15) Fiala, K. A., Abdel-Gawad, W., and Suo, Z. (2004) Pre-Steady-State Kinetic Studies of the Fidelity and Mechanism of Polymerization Catalyzed by Truncated Human DNA Polymerase *λ*. *Biochemistry 43*, 6751−6762.

(16) Fiala, K. A., and Suo, Z. (2004) Mechanism of DNA Polymerization Catalyzed by *Sulfolobus solfataricus* P2 DNA Polymerase IV. *Biochemistry 43*, 2116−2125.

(17) Joyce, C. M., and Benkovic, S. J. (2004) DNA polymerase fidelity: Kinetics, structure, and checkpoints. *Biochemistry 43*, 14317−14324.

(18) Fiala, K. A., Sherrer, S. M., Brown, J. A., and Suo, Z. (2008) Mechanistic consequences of temperature on DNA polymerization catalyzed by a Y-family DNA polymerase. *Nucleic Acids Res. 36*, 1990−2001.

(19) Xu, C., Maxwell, B. A., Brown, J. A., Zhang, L., and Suo, Z. (2009) Global conformational dynamics of a Y-family DNA polymerase during catalysis. *PLoS Biol. 7*, e1000225.

(20) Rothwell, P. J., Mitaksov, V., and Waksman, G. (2005) Motions of the fingers subdomain of Klentaq1 are fast and not rate limiting: Implications for the molecular basis of fidelity in DNA polymerases. *Mol. Cell 19*, 345−355.

(21) Allen, W. J., Rothwell, P. J., and Waksman, G. (2008) An intramolecular FRET system monitors fingers subdomain opening in Klentaq1. *Protein Sci. 17*, 401−408.

(22) Joyce, C. M., Potapova, O., DeLucia, A. M., Huang, X., Basu, V. P., and Grindley, N. D. F. (2008) Fingers-Closing and Other Rapid Conformational Changes in DNA Polymerase I (Klenow Fragment) and Their Role in Nucleotide Selectivity. *Biochemistry 47*, 6103−6116.

(23) Nakamura, T., Zhao, Y., Yamagata, Y., Hua, Y.-j., and Yang, W. (2012) Watching DNA polymerase *η* make a phosphodiester bond. *Nature 487*, 196−201.

(24) Kiefer, J. R., Mao, C., Braman, J. C., and Beese, L. S. (1998) Visualizing DNA replication in a catalytically active *Bacillus* DNA polymerase crystal. *Nature 391*, 304−307.

(25) Carey, P. R. (2006) Raman crystallography and other biochemical applications of Raman microscopy. *Annu. Rev. Phys. Chem. 57*, 527−554.

(26) Gong, B., Chen, J.-H., Yajima, R., Chen, Y., Chase, E., Chadalavada, D. M., Golden, B. L., Carey, P. R., and Bevilacqua, P. C. (2009) Raman crystallography of RNA. *Methods 49*, 101−111.

(27) Carey, P. R. (1982) *Molecular Biology: Biochemical Applications of Raman and Resonance Raman Spectroscopies*, Academic Press, New York.

(28) Maiti, N. C., Apetri, M. M., Zagorski, M. G., Carey, P. R., and Anderson, V. E. (2004) Raman Spectroscopic Characterization of Secondary Structure in Natively Unfolded Proteins: *α*-Synuclein. *J. Am. Chem. Soc. 126*, 2399−2408.

(29) Overman, S. A., and Thomas, G. J., Jr. (1999) Raman Markers of Nonaromatic Side Chains in an *α*-Helix Assembly: Ala, Asp, Glu, Gly, Ile, Leu, Lys, Ser, and Val Residues of Phage fd Subunits. *Biochemistry 38*, 4018−4027.

(30) Thomas, G. J., Jr., Benevides, J. M., Overman, S. A., Ueda, T., Ushizawa, K., Saitoh, M., and Tsuboi, M. (1995) Polarized Raman spectra of oriented fibers of A DNA and B DNA: Anisotropic and isotropic local Raman tensors of base and backbone vibrations. *Biophys. J. 68*, 1073−1088.

(31) Tsuboi, M., Suzuki, M., Overman, S. A., and Thomas, G. J., Jr. (2000) Intensity of the Polarized Raman Band at 1340−1345 cm^{-1} as an Indicator of Protein *α*-Helix Orientation: Application to Pf1 Filamentous Virus. *Biochemistry 39*, 2677−2684.

(32) Chen, Y., Basu, R., Gleghorn, M. L., Murakami, K. S., and Carey, P. R. (2011) Time-Resolved Events on the Reaction Pathway of Transcript Initiation by a Single-Subunit RNA Polymerase: Raman Crystallographic Evidence. *J. Am. Chem. Soc. 133*, 12544−12555.
(33) Cox, M. M., Doudna, J. A., and O'Donnell, M. (2012) *Molecular Biology. Principles and Practice*, W. H. Freeman and Co., New York.
(34) Vaisman, A., Ling, H., Woodgate, R., and Yang, W. (2005) Fidelity of Dpo4: Effect of metal ions, nucleotide selection and pyrophosphorolysis. *EMBO J. 24*, 2957−2967.
(35) Helfand, M. S., Totir, M. A., Carey, M. P., Hujer, A. M., Bonomo, R. A., and Carey, P. R. (2003) Following the Reactions of Mechanism-Based Inhibitors with β-Lactamase by Raman Crystallography. *Biochemistry 42*, 13386−13392.
(36) Padayatti, P. S., Helfand, M. S., Totir, M. A., Carey, M. P., Hujer, A. M., Carey, P. R., Bonomo, R. A., and van den Akker, F. (2004) Tazobactam Forms a Stoichiometric trans-Enamine Intermediate in the E166A Variant of SHV-1 β-Lactamase: 1.63 Å Crystal Structure. *Biochemistry 43*, 843−848.
(37) Basu, R. S., and Murakami, K. S. (2013) Watching the bacteriophage N4 RNA polymerase transcription by time-dependent soak-trigger-freeze X-ray crystallography. *J. Biol. Chem. 288*, 3305−3311.
(38) Torkabadi, H. H., Che, T., Shou, J., Shanmugam, S., Crowder, M. W., Bonomo, R. A., Pusztai-Carey, M., and Carey, P. R. (2013) Raman spectra of interchanging β-lactamase inhibitor intermediates on the millisecond time scale. *J. Am. Chem. Soc. 135*, 2895−2898.
(39) Chen, Y., Basu, R., Gleorn, M. L., Muakami, K. S., and Caey, P. R. (2011) Time-Resoled Evens on the Reaction Pathway of Transcrip Initiation by a Single-Subunit RNA Polymerase: Raman Crystallographic Evidence. *J. Am. Chem. Soc. 133*, 12544−12555.
(40) Basu, R. S., and Murakami, K. S. (2013) Watching the Bacteriophage N4 RNA Polymerase Transcription by Time-dependent Soak-trigger-freeze X-ray Crystallography. *J. Biol. Chem. 288*, 3305−3311.